

## MHD flow of a dusty fluid between two infinite parallel plates with temperature dependent physical properties under exponentially decaying pressure gradient

H.A. Attia<sup>1\*</sup>, A.L. Aboul-Hassan<sup>2</sup>, M.A.M. Abdeen<sup>2</sup>, A.El-Din Abdin<sup>3</sup>

<sup>1</sup> *Department of Engineering Mathematics and Physics, Faculty of Engineering, El-Fayoum University, El-Fayoum-63514, Egypt*

<sup>2</sup> *Department of Engineering Mathematics and Physics, Faculty of Engineering, Cairo University, Giza 12211, Egypt*

<sup>3</sup> *National Water Research Center, Ministry of Water Resources and Irrigation, Egypt*

Received May 29, 2013; revised July 4, 2014

In this study, the unsteady magnetohydrodynamic (MHD) flow and heat transfer of a dusty electrically conducting fluid between two infinite horizontal plates with temperature dependent physical properties are investigated. The fluid is acted upon by an exponentially decaying pressure gradient in the axial direction and an external uniform magnetic field perpendicular to the plates. The governing coupled momentum and energy equations are solved numerically by using the method of finite differences. The effects of the variable physical properties and the applied magnetic field on the velocity and temperature fields for both the fluid and dust particles are studied.

**Key words:** Two-phase flow, heat transfer, parallel plates, variable properties, numerical solution.

### INTRODUCTION

The flow and the heat transfer of dusty fluids in a channel have been studied by many authors [1-7]. The study of this type of flow gets its importance from its wide range of applications especially in the fields of fluidization, combustion, use of dust in gas cooling systems, centrifugal separation of matter from fluid, petroleum industry, purification of crude oil, electrostatic precipitation, polymer technology, and fluid droplets sprays. The flow of a dusty conducting fluid through a channel in the presence of a transverse magnetic field has a variety of applications in MHD generators, pumps, accelerators, and flowmeters. In these devices, the solid particles in form of ash or soot are suspended in the conducting fluid as a result of the corrosion and wear activities and/or the combustion processes in MHD generators and plasma MHD accelerators. The consequent effect of the presence of solid particles on the performance of such devices has led to studies of particulate suspensions in conducting fluids in the presence of externally applied magnetic field [8-13].

Most of the above mentioned studies are based on constant physical properties. More accurate prediction for the flow and heat transfer can be achieved by taking into account the variation of

these properties with temperature [14]. Klemp et al. [15] studied the effect of temperature dependent viscosity on the entrance flow in a channel in the hydrodynamic case. Attia and Kotb [16] studied the steady MHD fully developed flow and heat transfer between two parallel plates with temperature dependent viscosity. Later Attia [17] extended the problem to the transient state.

In the present work, the transient flow and heat transfer of an electrically conducting, viscous, incompressible dusty fluid with temperature-dependent viscosity and thermal conductivity are studied. The fluid is flowing between two electrically insulating infinite plates maintained at two constant but different temperatures. The fluid is acted upon by an exponentially decaying pressure gradient and an external uniform magnetic field perpendicular to the plates. The magnetic Reynolds number is assumed very small so that the induced magnetic field is neglected. It is assumed that the flow is laminar and the dust particles occupy a constant finite volume fraction. This configuration is a good approximation of some practical situations such as heat exchangers, flow meters, and pipes that connect system components. This problem is chosen due to its occurrence in many industrial engineering applications [18].

In general, there are two basic approaches for modeling two-phase fluid-particle flows. They are based on the Eulerian and the Lagrangian descriptions known from fluid mechanics. The

---

\* To whom all correspondence should be sent:  
E-mail: ah1113@yahoo.com

former treats both the fluid and the particle phases as interacting continua [19-21], while the latter treats only the fluid phase as a continuum with the particle phase being governed by the kinetic theory [22]. The present work employs the continuum approach and employs the dusty-fluid equations discussed by Marble [19].

The flow and temperature distributions of both the fluid and dust particles are governed by a coupled set of the momentum and energy equations. The Joule and viscous dissipations are taken into consideration in the energy equation. The governing coupled nonlinear partial differential equations are solved numerically by using finite differences. The effects of the external uniform magnetic field and of the variable viscosity and thermal conductivity on the time development of the velocity and temperature distributions for both the fluid and dust particles are discussed.

DESCRIPTION OF THE PROBLEM

In this paper, the dusty fluid is assumed to be flowing between two infinite horizontal electrically non-conducting stationary plates located at the  $y=\pm h$  planes and kept at two constant temperatures  $T_1$  for the lower plate and  $T_2$  for the upper plate with  $T_2>T_1$  so natural convection is eliminated. The dust particles are assumed to be spherical in shape and uniformly distributed throughout the fluid. The motion of the fluid is produced by an exponential decaying pressure gradient  $dP/dx = -Ge^{-\alpha x}$  in the  $x$ -direction, where  $G$  and  $\alpha$  are constants. This is an example of a time-dependent pressure gradient. Other forms of time-dependent pressure gradients may be considered in future work. A uniform magnetic field  $B_o$  is applied in the positive  $y$ -direction. Geometry of the problem is illustrated in Figure 1.

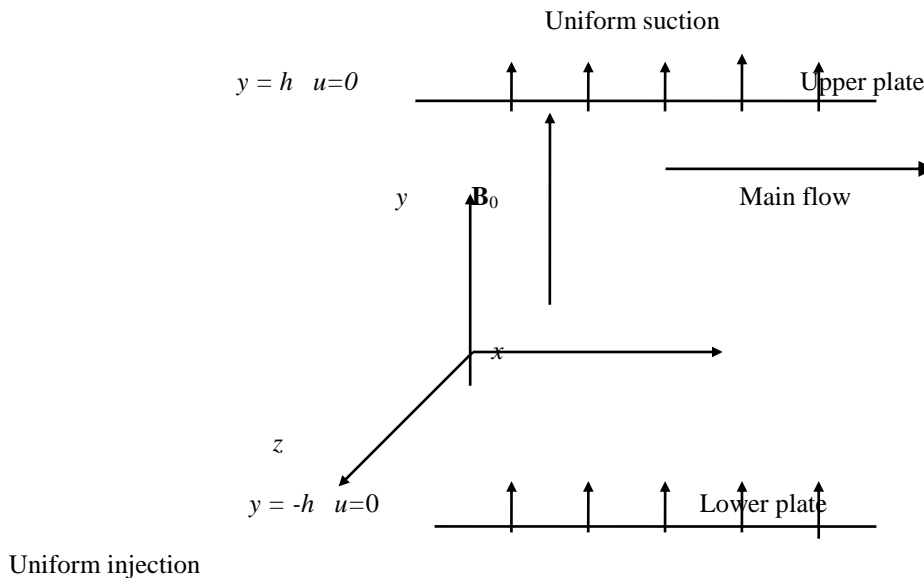


Fig. .1 The geometry of the problem

The fluid motion starts from rest at  $t=0$ , and the no-slip condition at the plates implies that the fluid and dust particles velocities vanish at  $y=\pm h$ . The initial temperatures of the fluid and of dust particles are assumed equal to  $T_1$ . The viscosity and the thermal conductivity of the fluid are taken to be temperature dependent. The viscosity is taken to vary exponentially with temperature whereas a linear dependence on temperature of the thermal conductivity is assumed. Since the plates are infinite in the  $x$  and  $z$ -directions, the physical variables are invariant in these directions and the problem is essentially one-dimensional with velocities  $u(y,t)$  and  $u_p(y,t)$  along the  $x$ -axis for fluid and particle phase respectively.

To formulate the governing equations for this investigation, the balance laws of mass and linear momentum are considered along with information about interfacial and external body forces and stress tensors for both phases. The balance laws of mass (for the fluid and particulate phases, respectively) may be written as

$$\partial_t \phi - \vec{\nabla} \cdot ((1 - \phi)\vec{V}) = 0, \tag{1a}$$

$$\partial_t \phi + \vec{\nabla} \cdot (\phi \vec{V}_p) = 0, \tag{1b}$$

where  $t$  is time,  $\phi$  is the particulate volume fraction,  $\vec{V}$  is the fluid-phase velocity vector, and  $\vec{V}_p$  is the particulate-phase velocity vector. The

fluid is assumed incompressible and the densities for both phases are assumed constant.

The balance laws of linear momentum (for the fluid and particulate phases, respectively) may be written as

$$\rho(1-\phi)(\partial_t \vec{V} + \vec{V} \cdot \nabla \vec{V}) = \nabla \cdot \vec{\varepsilon} - \vec{f} + \vec{b}, \quad (2a)$$

$$\rho_p \phi (\partial_t \vec{V}_p + \vec{V}_p \cdot \nabla \vec{V}_p) = \vec{f} + \vec{b}_p \quad (2b)$$

where  $\rho$  is the fluid-phase density,  $\vec{\varepsilon}$  is the fluid-phase stress tensor,  $\vec{f}$  is the interphase force per unit volume associated with the relative motion between the fluid and particle phases,  $\vec{b}$  is the fluid-phase body force per unit volume, and  $\vec{b}_p$  is the particle-phase body force per unit volume.

Along with Eqs. (1) and (2), the following constitutive equations are used

$$\vec{\varepsilon} = (1-\phi)(-P\vec{I} + \mu(\nabla \vec{V} + (\nabla \vec{V})^T)), \quad (3a)$$

$$\vec{f} = N\rho_p \phi (\vec{V} - \vec{V}_p), \quad (3b)$$

$$\vec{b} = \sigma(\vec{V} \wedge \vec{B}_o) \wedge \vec{B}_o, \quad (3c)$$

$$\vec{b}_p = \vec{0}, \quad (3d)$$

where  $P$  is the fluid pressure,  $\vec{I}$  is the unit tensor,  $\mu$  is the fluid dynamic viscosity,  $\mu_p$  is the particle-phase dynamic viscosity,  $N$  is the momentum transfer coefficient [24], which for spherical dust particles  $= \frac{6\pi\mu r}{m}$ ,  $r$  is the average radius of dust particles,  $m$  is the average mass of dust particles,  $\rho_p = \frac{4\pi r^3}{3m}$  is the material density of dust particles,  $\sigma$  is the electric conductivity of the fluid and a transposed  $T$  denotes the transpose of a second-rank tensor. In the present work it is assumed that the suspension is dilute and thus no particle-particle interaction exists [19]. In Eq. (3c) it is assumed that the magnetic Reynolds number  $Re_m = \sigma\mu L_o U_o$ , which is the ratio of the induced magnetic field to the applied external magnetic field, is very small and hence the induced magnetic field is neglected [23] and  $B_o$  is the only magnetic field in the problem. The quantities  $\mu L_o U_o$  are respectively the magnetic permeability of the fluid, the characteristic length, which in this case  $= h$ , and

the characteristic velocity of the fluid. It should be pointed out that in the present work the hydrodynamic interactions between the phases are limited to the drag force. This assumption is feasible when the particle Reynolds number is assumed to be small. Other interactions such as the virtual mass force [25], the shear force associated with the turbulent motion of dust particles [26], and the spin-lift force [27] are assumed to be negligible compared to the drag force [28]. To recapitulate, it is assumed that the flow is laminar, the fluid is incompressible, dust particles occupy a constant finite volume fraction, induced magnetic field is negligible, the virtual mass force, shear force, and spin lift force on dust particles are negligible.

Substituting Eqs. (3) into Eqs. (1) and (2) yields, after some arrangements

$$\rho \frac{\partial u}{\partial t} = Ge^{-\alpha y} + \frac{\partial}{\partial y} \left( \mu \frac{\partial u}{\partial y} \right) - \sigma B_o^2 u - \kappa N(u - u_p), \quad (4)$$

$$\frac{\partial u_p}{\partial t} = N(u - u_p), \quad (5)$$

where  $\kappa = \rho_p \phi / (1 - \phi)$ . The first three terms in the right-hand side of Eq. (4) are respectively the pressure gradient, viscous forces, and Lorentz force terms. The last term represents the force due to the relative motion between fluid and dust particles. The initial and boundary conditions on the velocity fields are respectively given by

$$t = 0 : u = u_p = 0. \quad (6a)$$

For  $t > 0$ , the no-slip condition at the plates implies that

$$y = -h : u = u_p = 0, \quad (6b)$$

$$y = h : u = 0, u_p = 0. \quad (6c)$$

Heat transfer takes place from the upper hot plate to the lower cold plate by conduction through the fluid, and there is heat generation due to both the Joule and viscous dissipations. Dust particles gain heat from the fluid by conduction through their surface. To describe the temperature distributions for both the fluid and dust particles, two energy equations are required, which are [29, 30]

$$\rho c \frac{\partial T}{\partial t} = \frac{\partial}{\partial y} \left( k \frac{\partial T}{\partial y} \right) + \mu \left( \frac{\partial u}{\partial y} \right)^2 + \sigma B_o^2 u^2 + \frac{\rho_p C_s}{\gamma_T} (T_p - T), \quad (7)$$

$$\frac{\partial T_p}{\partial t} = -\frac{1}{\gamma_T}(T_p - T), \tag{8}$$

where  $T$  is the temperature of the fluid,  $T_p$  is the temperature of the particles,  $c$  is the specific heat capacity of the fluid at constant volume,  $C_s$  is the specific heat capacity of the particles,  $k$  is the thermal conductivity of the fluid,  $\gamma_T$  is the temperature relaxation time =  $3Pr\gamma_p C_s / 2c$ ,  $\gamma_p$  is the velocity relaxation time =  $2\rho_{pr}^2/9\mu$ ,  $Pr$  is the Prandtl number =  $\mu_o c / k_o$ ,  $\mu_o$  and  $k_o$  are, respectively, the viscosity and thermal conductivity of the fluid at  $T_1$ . The last three terms in the right-hand side of Eq. (7) represent, respectively, the viscous dissipation, the Joule dissipation, and the heat conduction between the fluid and dust particles. The initial and boundary conditions of the temperature fields are

$$t \leq 0 : T = T_p = T_1, \tag{9a}$$

$$t > 0, y = -h : T = T_p = T_1, \tag{9b}$$

$$t > 0, y = h : T = T_p = T_2. \tag{9c}$$

The viscosity of the fluid is assumed to depend on temperature and is defined as,  $\mu = \mu_o f_1(T)$ . For practical reasons relevant to most fluids [15, 30, 31], the viscosity is assumed to vary exponentially with temperature. The function  $f_1(T)$  takes the form [13,14],  $f_1(T) = e^{-a(T-T_1)}$ . The parameter  $a$  is positive values for liquids such as water, benzene or crude oil. In some gases like air, helium or methane  $a$  is negative, that is the viscosity increases with temperature [9, 24, 30].

The thermal conductivity of the fluid is assumed to vary with temperature as  $k = k_o f_2(T)$ . We assume linear dependence of the thermal conductivity on temperature, that is,  $f_2(T) = 1 + b(T - T_1)$ , where the parameter  $b$  may be positive for some fluids such as air or water vapor or negative for others fluids such as liquid water or benzene [30, 31].

The problem is given more generality if the equations are written in the non-dimensional form. To do this, define the following non-dimensional quantities,

$$(\hat{x}, \hat{y}) = \left(\frac{x}{h}, \frac{y}{h}\right),$$

$$\hat{t} = \frac{t\mu_o}{\rho h^2},$$

$$(\hat{u}, \hat{u}_p) = \left(\frac{u\rho h}{\mu_o}, \frac{u_p\rho h}{\mu_o}\right),$$

$$\hat{T} = \frac{T - T_1}{T_2 - T_1}, \hat{T}_p = \frac{T_p - T_1}{T_2 - T_1},$$

$$\hat{G} = \frac{Gh^3\rho}{\mu_o^2},$$

$\hat{a} = a(T_2 - T_1)$  is the viscosity parameter,

$\hat{b} = b(T_2 - T_1)$  is the thermal conductivity parameter,

$$\hat{f}_1(\hat{T}) = e^{-\hat{a}\hat{T}},$$

$$\hat{f}_2(\hat{T}) = 1 + \hat{b}\hat{T},$$

$Ha^2 = \sigma B_o^2 h^2 / \mu_o$ ,  $Ha$  is the Hartmann number,

$R = \kappa N h^2 / \mu_o$  is the particle concentration parameter,

$G_1 = \mu_o / N\rho h^2$  is the particle mass parameter,

$Pr = \mu_o c / k_o$  is the Prandtl number,

$Ec = \mu_o^2 / \rho^2 h^2 c_p (T_2 - T_1)$  is the Eckert number.

$L_o = \rho h^2 / \mu_o \gamma_T$  is the temperature relaxation time parameter.

In terms of the above non-dimensional variables and parameters Eqs. (4)-(9) take the form (hats are dropped for convenience)

$$\frac{\partial u}{\partial t} = Ge^{-\hat{a}t} + f_1(T) \frac{\partial^2 u}{\partial y^2} + \frac{\partial f_1(T)}{\partial y} \frac{\partial u}{\partial y} - Ha^2 u - R(u - u_p) \tag{10}$$

$$\frac{\partial u_p}{\partial t} = \frac{1}{G_1}(u - u_p) \tag{11}$$

$$t \leq 0 : u = u_p = 0. \tag{12a}$$

$$t > 0, y = -1 : u = u_p = 0, \tag{12b}$$

$$t > 0, y = 1 : u = 1, u_p = 0, \tag{12c}$$

$$\frac{\partial T}{\partial t} = \frac{1}{Pr} f_2(T) \frac{\partial^2 T}{\partial y^2} + \frac{1}{Pr} \frac{\partial f_2(T)}{\partial y} \frac{\partial T}{\partial y} + Ec f_1(T) \left( \frac{\partial u}{\partial y} \right)^2 + Ec Ha^2 u^2 + \frac{2R}{3Pr} (T_p - T), \quad (13)$$

$$\frac{\partial T_p}{\partial t} = -L_o (T_p - T), \quad (14)$$

$$t \leq 0 : T = T_p = 0, \quad (15a)$$

$$t > 0, y = -1 : T = T_p = 0, \quad (15b)$$

$$t > 0, y = 1 : T = T_p = 1, \quad (15c)$$

Equations (10), (11), (13), and (14) represent a system of coupled, nonlinear partial differential equations which may be solved numerically under the initial and boundary conditions (12) and (15) using the finite difference approximations. The Crank-Nicolson implicit method is used [32]. Finite difference equations relating the variables are obtained by writing the equations at the mid point of the computational cell and then replacing the different terms by their second order central difference approximations in the y-direction. The diffusion term is replaced with the average of the central differences at two successive time levels. The nonlinear terms are first linearized and then an iterative scheme is used at every time step to solve the linearized system of difference equations. The solution at a certain time step is chosen as an initial guess for next time step and the iterations are continued till convergence, within a prescribed accuracy. Finally, the resulting block tri-diagonal system is solved using the generalized Thomas-algorithm [32]. We define the variables  $A = \partial u / \partial y$  and  $H = \partial \theta / \partial y$  to reduce the second order differential Eqs. (10) and (13) to first order differential equations, and an iterative scheme is used at every time step to solve the linearized system of difference equations. In the numerical solution some parameters are not varied and given the following fixed values:  $R=0.5$ ,  $G_1=0.8$ ,  $G=5$ ,  $\alpha=1$ ,  $Pr=1$ ,  $Ec=0.2$ , and  $L_o=0.7$ . Step sizes  $\Delta t=0.001$  and  $\Delta y=0.01$  for time and space, respectively are chosen. Smaller step sizes do not show any significant change in the results. The iterative scheme continues until the fractional difference between two successive iterations becomes less than a specified small value. Convergence of the scheme is assumed when all of the unknowns  $u$ ,  $A$ ,  $T$  and  $H$  for the last two approximations differ from unity by less than  $10^{-6}$  for all values of  $y$  in  $-1 < y < 1$  at every time step.

The required accuracy is usually reached after about 7 iterations. It should be mentioned that the results obtained herein reduce to those reported by Singh [8] and Aboul-Hassan et al. [12] for the case of fluid with constant properties. These comparisons lend confidence in the accuracy and correctness of the solutions presented.

A linearization technique is first applied to replace the nonlinear terms at a linear stage, with the corrections incorporated in subsequent iterative steps until convergence is reached. Then the Crank-Nicolson implicit method is used at two successive time levels [26]. An iterative scheme is used to solve the linearized system of difference equations. The solution at a certain time step is chosen as an initial guess for next time step and the iterations are continued till convergence, within a prescribed accuracy. Finally, the resulting block tri-diagonal system is solved using the generalized Thomas-algorithm [26]. Finite difference equations relating the variables are obtained by writing the equations at the mid point of the computational cell and then replacing the different terms by their second order central difference approximations in the y-direction. The diffusion terms are replaced by the average of the central differences at two successive time-levels. The computational domain is divided into meshes each of dimension  $\Delta t$  and  $\Delta y$  in time and space, respectively. We define the variables  $A = \partial u / \partial y$ ,  $B = \partial w / \partial y$  and  $H = \partial \theta / \partial y$  to reduce the second order differential Eqs. (9), (10) and (12) to first order differential equations, and an iterative scheme is used at every time step to solve the linearized system of difference equations. All calculations are carried out for the non-dimensional variables and parameters given by,  $G=5$ ,  $Pr=1$ , and  $Ec=0.2$  where  $G$  is related to the externally applied pressure gradient and where the chosen given values for  $Pr$  and  $Ec$  are suitable for steam or water vapor. Grid-independence studies show that the computational domain  $0 < t < \infty$  and  $-1 < y < 1$  is divided into intervals with step sizes  $\Delta t=0.0001$  and  $\Delta y=0.005$  for time and space respectively. Smaller step sizes do not show any significant change in the results. Convergence of the scheme is assumed when all of the unknowns  $u$ ,  $w$ ,  $A$ ,  $B$ ,  $\theta$  and  $H$  for the last two approximations differ from unity by less than  $10^{-6}$  for all values of  $y$  in  $-1 < y < 1$  at every time step. Less than 7 approximations are required to satisfy this convergence criteria for all ranges of the parameters studied here.

RESULTS AND DISCUSSIONS

Figures 2a, 2b, 3a, and 3b show the effect of the viscosity parameter  $a$  on the time development of the velocities  $u$  and  $u_p$ , and the temperatures  $T$  and  $T_p$ , respectively, at the center of the channel ( $y=0$ ) for  $Ha = 0$  and  $b = 0$ . Figures 1a and 1b indicate that increasing  $a$  increases  $u$  and  $u_p$  and increases the time required to approach the steady state. This is a result of decreasing the viscous forces. The effect of the parameter  $a$  on the steady state time is more pronounced for positive values of  $a$  than for

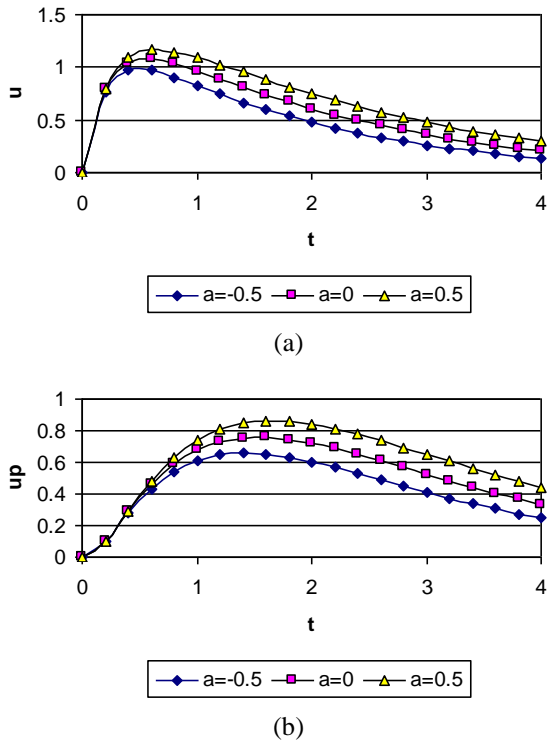


**Fig. 2.** Effect of the viscosity parameter  $a$  on the time variation of: (a) the fluid velocity  $u$  at the center of the channel ( $y=0$ ); (b) the particle phase velocity  $u_p$  at the center of the channel ( $y=0$ ). ( $Ha=0$ )

Figures 4a, 4b, 5a, and 5b present the effect of the viscosity parameter  $a$  on the time development of  $u$ ,  $u_p$ ,  $T$  and  $T_p$ , respectively, at the centre of the channel ( $y=0$ ) for  $Ha=1$  and  $b=0$ . The introduction of the uniform magnetic field adds one resistive term to the momentum equation and the Joule dissipation term to the energy equation. As shown in Figures 4a, and 4b the magnetic field results in

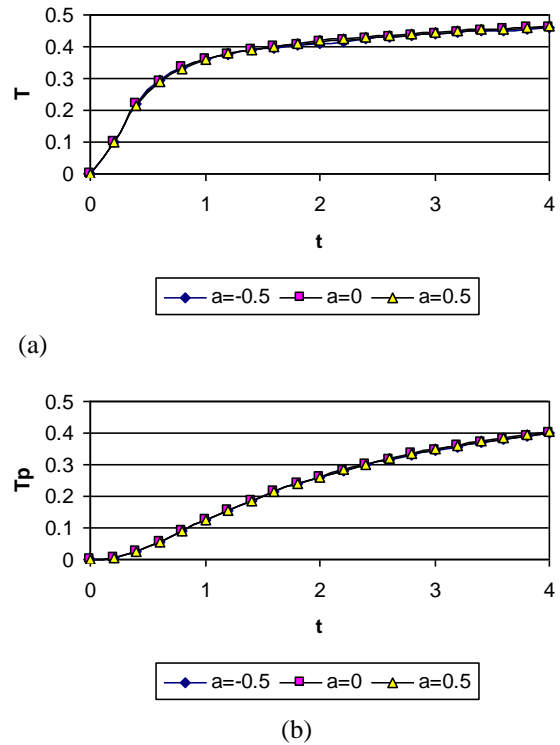
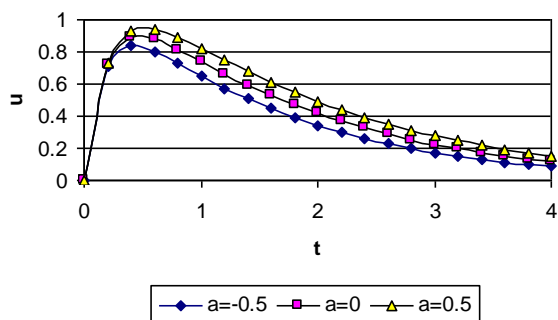
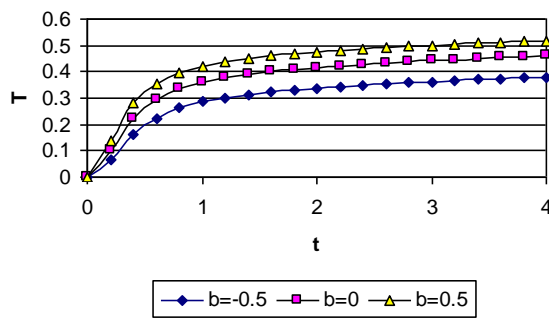


**Fig. 3.** Effect of the viscosity parameter  $a$  on the time variation of: (a) the fluid temperature  $T$  at the center of the channel ( $y=0$ ); (b) the particle phase temperature  $T_p$  at the center of the channel ( $y=0$ ). ( $Ha=0$ ).

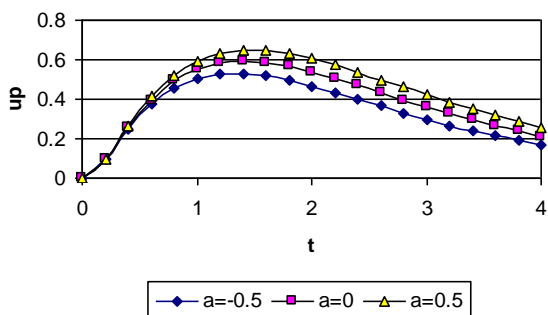
a reduction in the velocities  $u$  and  $u_p$  and their steady state times for all values of  $a$  due to its damping effect. Figures 5a, and 5b confirm that the parameter  $a$  has a negligible effect on temperature and the viscous dissipation is negligible. Comparing with Figures 3 and 5, it is observed that the temperature are slightly higher in the presence of the magnetic field ( $Ha = 1$ ). This means that the Joule dissipation is small but now negligible. Notice that  $u$  reaches the steady state faster than  $u_p$  which is expected because the fluid velocity is the source for the dust particles velocity. Figures 3a and 3b show that the viscosity parameter  $a$  has a negligible effect on temperature. This means that the viscous dissipation is negligible. Of course there is no Joule dissipation when  $Ha = 0$ . The time at which  $T_p$  reaches the steady state is longer than that for  $T$  since  $T_p$  always follows  $T$ .



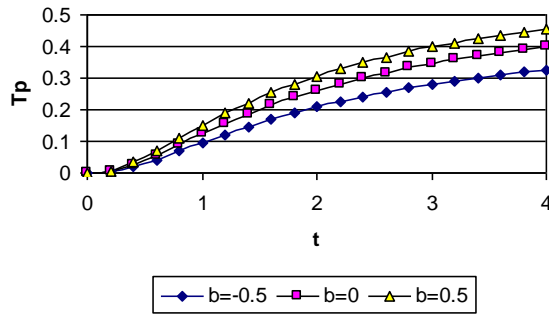
(a)



(a)



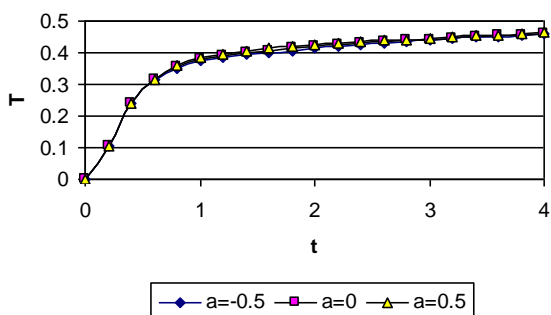
(b)



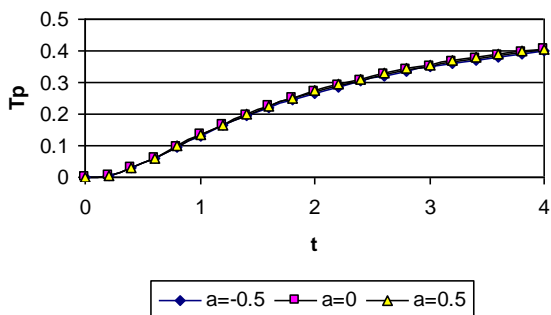
(b)

**Fig. 4.** Effect of the viscosity parameter  $a$  on the time variation of: (a) the fluid velocity  $u$  at the center of the channel ( $y=0$ ); (b) the particle phase velocity  $u_p$  at the center of the channel ( $y=0$ ). ( $Ha=1$ ).

**Fig. 6.** Effect of the thermal conductivity parameter  $b$  on the time variation of: (a) the fluid temperature  $T$  at the center of the channel ( $y=0$ ); (b) the particle phase temperature  $T_p$  at the center of the channel ( $y=0$ ). ( $Ha=0$ )



(a)

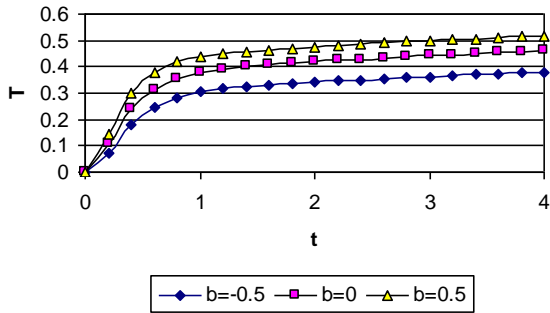


(b)

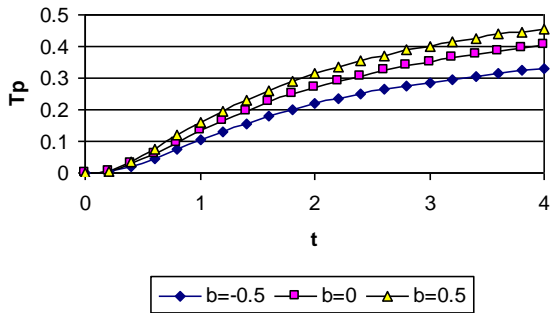
**Fig. 5.** Effect of the viscosity parameter  $a$  on the time variation of: (a) the fluid temperature  $T$  at the center of the channel ( $y=0$ ); (b) the particle phase temperature  $T_p$  at the center of the channel ( $y=0$ ). ( $Ha=1$ )

Figures 6a, and 6b show the effect of the thermal conductivity parameter  $b$  on the time development of the temperatures  $T$  and  $T_p$ , respectively, at the center of the channel ( $y=0$ ) for  $Ha=0$  and  $a=0$ . The figures show that increasing  $b$  increases  $T$  and  $T_p$  as a result of increasing the thermal conductivity. In Figure 6a it is interesting that the steady state value of the fluid temperature at the center of the channel exceeds 0.5 for positive values of  $b$  although the Joule and viscous dissipations are absent. The reason is that the thermal conductivity in the upper half of the channel is more than in the lower half if  $b$  is positive.

Figures 7a, and 7b present the effect of the thermal conductivity parameter  $b$  on the time development of the temperatures  $T$  and  $T_p$ , respectively, at the center of the channel ( $y=0$ ) for  $Ha=1$  and  $a=0$ . The introduction of the magnetic field increases both  $T$  and  $T_p$  for all values of  $b$  due to the increase in the dissipation.



(a)



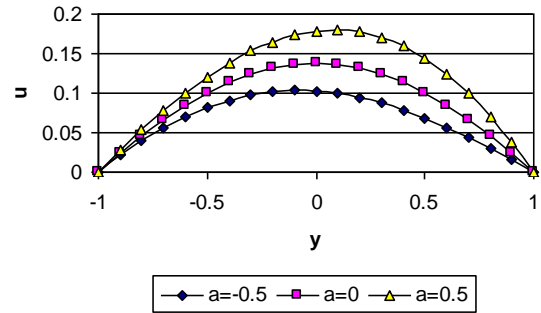
(b)

**Fig. 7.** Effect of the thermal conductivity parameter  $b$  on the time variation of: (a) the fluid temperature  $T$  at the center of the channel ( $y=0$ ); (b) the particle phase temperature  $T_p$  at the center of the channel ( $y=0$ ). ( $Ha=1$ )

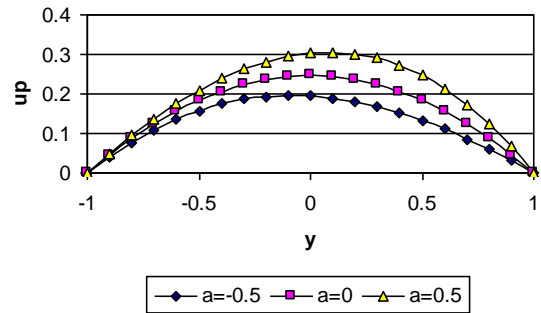
Figures 8a, 8b, 9a, and 9b present the effect of the viscosity parameter  $a$  on the profiles of the velocities  $u$  and  $u_p$ , and the temperatures  $T$  and  $T_p$  for  $Ha=1$  and  $b=0$  at  $t=6$ .

Increasing  $a$  increases the velocity and displaces the peak of the velocity profile towards the upper plate where the viscosity is less. This effect is akin to the displacement of the peak of the velocity distribution where there is suction at one plate and injection at the other plate. Positive values of  $a$  correspond to a suction velocity from the cold plate to the hot plate, while negative values of  $a$  correspond to a suction velocity from the hot plate to the cold plate. Figures 9a, and 9b show that increasing  $a$  increases the temperatures  $T$  and  $T_p$  for all values of  $y$ . It is clear from Figures 8, and 9 that the effect of the parameter  $a$  on the velocities is more pronounced than on the temperatures.

Figures 10a, and 10b present the effect of the thermal conductivity parameter  $b$  on the temperature profiles at  $t=0$ , for  $Ha=1$  and  $a=0$ . The figures indicate that increasing  $b$  increases  $T$  and  $T_p$  for all values of  $y$ . This because increasing  $b$  means that the thermal conductivity near the hot plate gets more than near the cold plat.

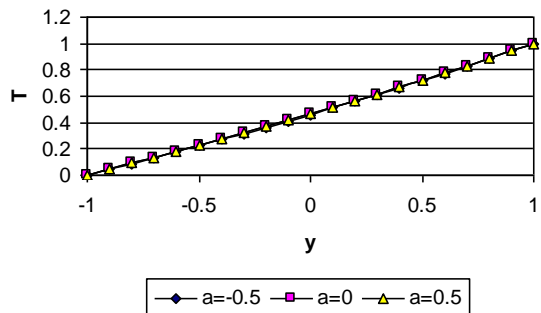


(a)

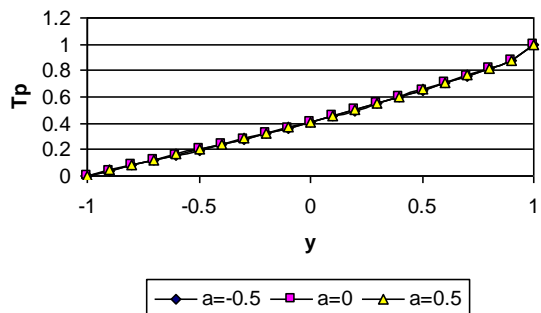


(b)

**Fig. 8.** Effect of the viscosity parameter  $a$  on the profile of: (a) the fluid velocity  $u$  at  $t=6$ ; (b) the particle phase velocity  $u_p$  at  $t=6$ . ( $Ha=1$ )

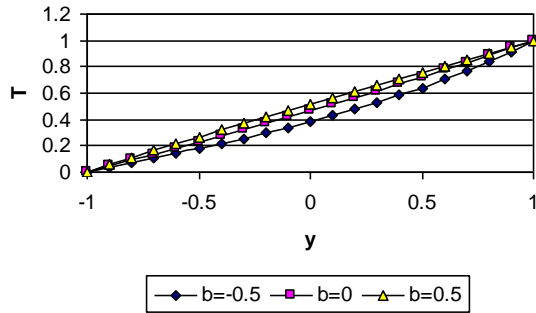


(a)

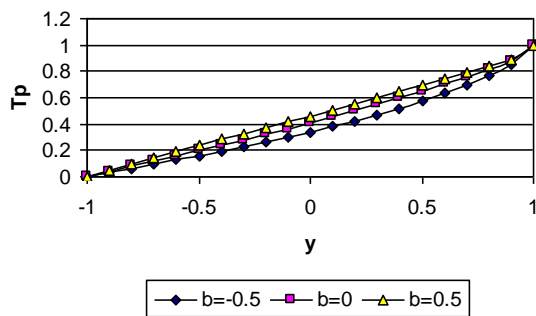


(b)

**Fig. 9.** Effect of the viscosity parameter  $a$  on the profile of: (a) the fluid temperature  $T$  at  $t=6$ ; (b) the particle phase temperature  $T_p$  at  $t=6$ . ( $Ha=1$ )



(a)



(b)

**Fig. 10.** Effect of the thermal conductivity parameter  $b$  on the profile of: (a) the fluid temperature  $T$  at  $t = 6$ ; (b) the particle phase temperature  $T_p$  at  $t = 6$ . ( $Ha=1$ ).

**Table 1.** Variation of  $u$  at  $y=0$  for various values of  $a$  and  $b$  at  $t=6$  ( $Ha=1$ )

$u$	$a=-0.5$	$a=-0.1$	$a=0.0$	$a=0.1$	$a=0.5$
$b=-0.5$	0.0882	0.0862	0.0857	0.0854	0.0842
$b=-0.1$	0.1096	0.1091	0.1089	0.1089	0.1086
$b=0.0$	0.1154	0.1154	0.1154	0.1154	0.1154
$b=0.1$	0.1214	0.1219	0.1220	0.1221	0.1225
$b=0.5$	0.1473	0.1502	0.1508	0.1513	0.1532

**Table 2.** Variation of  $u_p$  at  $y=0$  for various values of  $a$  and  $b$  at  $t=6$  ( $Ha=1$ )

$u_p$	$a=-0.5$	$a=-0.1$	$a=0.0$	$a=0.1$	$a=0.5$
$b=-0.5$	0.1716	0.1683	0.1676	0.1669	0.1651
$b=-0.1$	0.2029	0.2022	0.2020	0.2019	0.2014
$b=0.0$	0.2112	0.2112	0.2112	0.2112	0.2112
$b=0.1$	0.2197	0.2204	0.2206	0.2207	0.2212
$b=0.5$	0.2549	0.2588	0.2597	0.2604	0.2629

**Table 3.** Variation of  $T$  at  $y=0$  for various values of  $a$  and  $b$  at  $t=6$  ( $Ha=1$ )

$T$	$a=-0.5$	$a=-0.1$	$a=0.0$	$a=0.1$	$a=0.5$
$b=-0.5$	0.3782	0.4440	0.4587	0.4723	0.5149
$b=-0.1$	0.3799	0.4455	0.4601	0.4736	0.5159
$b=0.0$	0.3803	0.4459	0.4605	0.4739	0.5163
$b=0.1$	0.3807	0.4463	0.4609	0.4743	0.5166
$b=0.5$	0.3829	0.4482	0.4627	0.4761	0.5181

**Table 4.** Variation of  $T_p$  at  $y=0$  for various values of  $a$  and  $b$  at  $t=6$  ( $Ha=1$ ).

$T_p$	$a=-0.5$	$a=-0.1$	$a=0.0$	$a=0.1$	$a=0.5$
$b=-0.5$	0.3271	0.3962	0.3998	0.4125	0.4536
$b=-0.1$	0.3296	0.3886	0.4021	0.4148	0.4557
$b=0.0$	0.3303	0.3892	0.4028	0.4154	0.4563
$b=0.1$	0.3309	0.3899	0.4034	0.4160	0.4568
$b=0.5$	0.3340	0.3929	0.4063	0.4188	0.4593

Tables 1-4 present the variation of  $u$ ,  $u_p$ ,  $T$ , and  $T_p$ , respectively, at the center of the channel ( $y=0$ ) at  $t=6$  for various values of  $a$  and  $b$  and for  $Ha=1$ . It is clear that increasing  $a$  increases the temperatures for both the fluid and dust particle for all values of  $b$ . However, its effect on the velocities depends on the value of  $b$ . For negative  $b$ , increasing  $a$  decreases  $u$  and  $u_p$  but for positive  $b$ , increasing  $a$  increases them. Increasing the parameter  $b$  increases the velocities  $u$  and  $u_p$  and the temperatures  $T$  and  $T_p$  for all values of  $a$ .

### CONCLUSIONS

In this paper the transient MHD flow and heat transfer of a dusty and electrically conducting fluid are studied in the presence of an external uniform magnetic field taking into consideration the variations of the viscosity and thermal conductivity of the fluid with temperature. The variation of the viscosity of the fluid with temperature has an apparent effect on the velocity of both the fluid and dust particles. The peak of the velocity distribution displaces from the center of the channel towards regions of less viscosity. Changing the viscosity has a negligible effect on temperatures and it is inferred that the viscous dissipation is negligible. Variation of the thermal conductivity of the fluid with temperature has a pronounced effect on temperature distributions. Temperatures shift towards the temperature of the plate near which the thermal conductivity is higher. Increasing the magnetic field decreases the velocity for both phases at all positions and times. It also produces a small increase in temperature and it is inferred that the Joule dissipation is small but not negligible.

### REFERENCES

1. P.G. Saffman, *J. Fluid Mech.*, **13**, 120 (1962).
2. R.K.Gupta, S.C. Gupta, *J. Appl. Mathem.&Physics*, **27**, 119 (1976).
3. V.R. Prasad, N.C.P. Ramacharyulu, *Def. Sci. J.*, **30**, 125 (1979).
4. L.A. Dixit, *Ind. J. Theor. Physics*, **28**, 129 (1980).
5. A.K. Ghosh, D.K. Mitra, *Rev. Roum. Phys.*, **29**, 631 (1984).

6. H.A. Attia, M.A.M. Abdeen, *J. Theor. Appl. Mech.*, **51**, 53 (2013).
7. H.A. Attia, M.A.M. Abdeen, A. El-Din Abdin, *J. Eng. Physics & Thermophysics*, **86**, 677 (2013).
8. K.K. Singh, *Ind. J. Pure & Appl. Mathem.* **8**, 1124 (1976).
9. P. Mitra, P. Bhattacharyya, *Acta Mechanica*, **39**, 171 (1981).
10. K. Borkakotia, A. Bharali, *Quart. Appl. Mathem.*, 461 (1983).
11. A.A. Megahed, A.L. Aboul-Hassan, H. Sharaf El-Din, Proc. Fifth Miami international Symposium on Multi-Phase Transport and Particulate Phenomena, Miami, Florida, USA, vol. 3, pp. 111, 1988.
12. A.L. Aboul-Hassan, H. Sharaf El-Din, A.A. Megahed, Proc. First International Conference of Engineering Mathematics and Physics, Cairo, pp. 723-734, 1991.
13. H.A. Attia, K.M. Ewis, I.H. Abd Elmaksoud, M.A. M. Abdeen, *J. Physical Chem. A*, **86**, 141 (2012).
14. H. Herwig, G. Wicken, *Waerme und Stoffuebertragung*, **20**, 47 (1986).
15. K. Klemp, H. Herwig, M. Selmann, Proc. Third International Congress of Fluid Mechanics, Cairo, Egypt, vol. 3, pp. 1257-1266, 1990.
16. H.A. Attia, N.A. Kotb., *Acta Mechanica*, **117**, 215 (1996).
17. H.A. Attia, *Mech. Res. Commun.*, **26**, 115 (1999).
18. K.R. Rajagopal, Tao, L., *World Scientific*, 1995.
19. F.E. Marble, *Ann. Rev. Fluid Mech.*, **2**, 397 (1970).
20. S.L. Soo, *Multiphase fluid dynamics*, Science Press, New York, 1990.
21. M. Ishii, *Thermo-fluid dynamics Theory of Two-Phase flow*, Eyrolles, Paris, 1975.
22. A. Berlemont, *Int. J. Multiphase Flow*, **16**, 19 (1990).
23. G.W. Sutton, A. Sherman, *Engineering Magneto-hydrodynamics*, McGraw-Hill, 1965.
24. A.J. Chamkha, *Int. J. Engng. Sci.*, **33**, 437 (1995).
25. N. Zuber, *Chem. Eng. Sci.*, **19**, 897 (1964).
26. P.G. Saffman, *J. Fluid Mech.*, **22**, 385 (1965).
27. S.I. Rubinow, J.B. Keller, *J. Fluid Mech.*, **11**, 447 (1961).
28. N. Apazidis, *Int. J. Multiphase Flow*, **11**, 675 (1985).
29. A.J. Chamkha, *Appl. Math. Modelling*, **21**, 287 (1997).
30. H. Schlichting, *Boundary layer theory*, McGraw-Hill, 1968.
31. M.F. White, *Viscous fluid flow*, McGraw-Hill, 1991.
32. W.F. Ames, *Numerical solutions of partial differential equations*, Second Edition, Academic Press, New York, 1977.

## МАГНИТОХИДРОДИНАМИЧНО ТЕЧЕНИЕ НА ЗАПРАШЕН ФЛУИД МЕЖДУ ДВЕ БЕЗКРАЙНИ УСПОРЕДНИ ПЛОСКОСТИ С ТЕМПЕРАТУРНО ЗАВИСИМИ ФИЗИЧНИ СВОЙСТВА ПРИ ЕКСПОНЕНЦИАЛНО ЗАТИХВАЩ ГРАДИЕНТ НА НАЛЯГАНЕТО

Х.А. Атия<sup>1\*</sup>, А.Л. Абул-Хасан<sup>2</sup>, М.А.М. Абдиин<sup>2</sup>, А. Ел-Дин Абдин<sup>3</sup>

<sup>1</sup> Департамент по инженерство, математика и физика, Факултет по инженерство, Университет в Ел-Фаюм, Ел-Фаюм 63514, Египет

<sup>2</sup> Департамент по инженерство, математика и физика, Факултет по инженерство, Университет в Кайро, Гиза 12211, Египет

<sup>3</sup> Национален център по водни изследвания, Министерство на водните проблеми и напояването, Египет

Постъпила на 29 май, 2013 г.; коригирана на 4 юли, 2013 г.

(Резюме)

В тази работа е изследвано нестационарното магнитохидродинамично течение (МНД) и топлообмена в запрашен електропроводящ флуид между две безкрайни успоредни плоскости при температурно зависими физични свойства. Флуидът се намира под действието експоненциално затихващ градиент на налягането по оста на течението и при хомогенно външно магнитно поле перпендикулярно на плоскостите. Спрегнатите уравнения на движението и на топлопроводността са решени числено по метода на крайните разлики. Изследван е и ефекта на променливите физични параметри и на приложеното магнитно поле върху скоростта на течението и температурното поле за флуида и за праховите частици.